

# Carbon Isotopic Evidences for Gas Hydrate Release and Its Significance on Seasonal Wetland Methane Emissions in the Qilian Mountains Permafrost

xiaoqian li

School of Environmental Studies, China University of Geosciences

Jianwei Xing

School of Environmental Studies, China University of Geosciences

Shouji Pang (✉ [psj0409@163.com](mailto:psj0409@163.com))

The Key Laboratory of Unconventional Oil & Gas Geology, China Geological Survey

Youhai Zhu

The Key Laboratory of Unconventional Oil & Gas Geology, China Geological Survey

Shuai Zhang

Oil and Gas Survey, China Geological Survey

Rui Xiao

Oil and Gas Survey, China Geological Survey

---

## Research Article

**Keywords:** Carbon isotopic, emissions, Qilian Mountains

**Posted Date:** March 4th, 2021

**DOI:** <https://doi.org/10.21203/rs.3.rs-264090/v1>

**License:** © ⓘ This work is licensed under a Creative Commons Attribution 4.0 International License.

[Read Full License](#)

---

# Abstract

Wetland methane emissions in the permafrost regions of the Qinghai-Tibet Plateau is more sensitive to climate warming and can result in a positive climate feedback. Natural gas hydrate, as a potential methane source, may play a pivotal role in wetland methane emission in the permafrost regions. However, it was lacking of evidence. To determine the role of gas hydrate release in wetland methane emission, the two-year field monitoring of methane emitted from a hydrate drilling well, in near-surface soil free gas and low-level air was conducted at a typical gas hydrate reservoir in the Qilian Mountains permafrost. The carbon isotope fractionation between  $\text{CO}_2$  and  $\text{CH}_4$  ( $\epsilon_C$ ) associated with carbon isotopic composition of methane ( $\delta^{13}\text{C}_{\text{CH}_4}$ ) is used as a good tracer to identify methane sources of thermogenic origin or of microbial origin. The monitoring results of the gas hydrate drilling well DK-8 indicated a notable release of the deep gas hydrates occurred in April- May and resulted in the increase of methane content in low-level air. The significance of gas hydrate release in the permafrost region on local wetland methane emission as well as low-level air methane was confirmed by the seasonal variation of methane source of near-surface soil fluxes and low-level air. The thermogenically derived methane were identified as the dominant methane source in autumn and winter compared with increasing contribution of microbially derived methane in summer. The carbon isotopic signatures of tracing methane sources can provide more reliable evidence for gas hydrate release and its effect on the wetland methane emission in the Qilian Mountains permafrost.

## Introduction

Methane ( $\text{CH}_4$ ) is an important greenhouse gas that provides the second largest contribution to historical global warming, with stronger climate warming potential than carbon dioxide ( $\text{CO}_2$ )<sup>1</sup>. Global atmospheric methane concentrations have increased rapidly since 2007 at a renewed growth rate of  $6.9 \pm 2.7 \text{ ppb yr}^{-1}$ <sup>2</sup>. Wetland methane emissions, the largest natural source in the global  $\text{CH}_4$  budget, plays an emerging role in driving 21st century climate change<sup>3</sup>. Carbon pools in permafrost regions represent a large reservoir vulnerable to climate change, driving a positive feedback to a warming climate<sup>4-8</sup>. Methane production in thawing permafrost is key to the greenhouse gas budget on climate-relevant timescales<sup>9</sup>. Therefore, wetland methane emission process strongly associated with wetland carbon cycling in permafrost regions is of great significance to understand climate feedback and mitigate global warming.

The Qinghai-Tibet Plateau is the largest high-altitude permafrost region on Earth, with a wetland area covering approximately  $130,000 \text{ km}^2$ <sup>10</sup>. Permafrost wetlands in the Qinghai-Tibet Plateau have received considerable attention, not only because the effects of climate warming on carbon ecosystems and wetlands emission are higher sensitive at high latitudes<sup>11-15</sup>, but also because this region holds vast amounts of soil organic carbon<sup>16-18</sup> stored in permafrost as well as thermogenic hydrocarbons in form of gas hydrates<sup>19-21</sup>. Climate warming has likely similar effects on greenhouse gases production in deep permafrost as in surface soils<sup>14</sup>. The interaction of wetland emission, permafrost thawing and

destabilization of gas hydrates, and their combined response to and effect on the climate warming, make methane emission of the Qinghai-Tibet Plateau unique and complex. Actually, the increase rate of atmospheric background methane concentration in the Qinghai-Tibet Plateau is significantly higher than the global average<sup>22</sup>. Therefore, sources identification of wetland methane emissions is of great significance to understand processes and mechanisms of wetland methane emissions in the permafrost regions in the Qinghai-Tibet Plateau.

Nature gas hydrates were first observed in 2008 in the Muli permafrost regions of the northeastern Qinghai-Tibet Plateau, mainly occurring in the pores and fissures of fine-grained sandstones, siltstones, mudstones, and dunnet shales of the Middle Jurassic Jiangcang Formation<sup>19</sup>. Gas hydrate and its associated anomalies generally appear at depths of 133–396 m below the permafrost base<sup>23</sup>. Natural gas hydrate, as a potential carbon pool, may cause massive methane leaking when stability conditions change and impose significant impacts on global carbon cycling and climate warming<sup>24–28</sup>. There is still some debate on the extent to which methane hydrate release is responsible for the past extreme warming events, such as the Cretaceous–Tertiary (K/T) boundary extinction event, the Palaeocene–Eocene thermal maximum (PETM) and the Quaternary glacial to interglacial cycles. Nevertheless, there is concern that global warming may lead to hydrate instability and an enhanced CH<sub>4</sub> flux to the atmosphere. Previous studies about gas hydrate in the Qinghai-Tibet Plateau indicated that the hydrocarbon gases in gas hydrates can effuse towards the land surface through microseepage<sup>29</sup> and may have an impact on the surface carbon circulation system, forming a key source of wetland methane emissions<sup>19,30–32</sup>. Until now there is only one recent study<sup>32</sup> that provided evidence of gas hydrate release as a new source of methane emissions from wetland soils in permafrost regions of the Qinghai-Tibet Plateau, which was identified by four high methane emission fluxes of 10.4 ~ 76.0 mg/m<sup>-2</sup> h<sup>-1</sup> and  $\delta^{13}\text{C}_{\text{CH}_4}$  values between -48.0‰ and -42.2‰ in the soil free gas during August. However, the magnitude and timing of gas hydrate release and its impact on wetland methane emission and atmospheric methane concentration in the Qinghai-Tibet Plateau remains not fully understood. Further studies to distinguish sources of wetland methane emission and atmospheric methane are needed.

Stable isotope signal of methane is frequently related to its sources. The gases of gas hydrates from the Muli permafrost regions in the Qinghai-Tibet Plateau are mainly of thermogenic origin<sup>33</sup>, with a  $\delta^{13}\text{C}_{\text{CH}_4}$  value ranging from -52.7‰ to -31.3‰. The thermogenic methane is generally enriched in <sup>13</sup>C compared with bacterial methane that has  $\delta^{13}\text{C}_{\text{CH}_4}$  values more negative than -50‰ and up to -100‰. The carbon isotope signatures of methane are useful to distinguish methane sources of thermogenic or biogenic origin. But situations, such as mixing of different natural gases or where extreme substrate depletion and CH<sub>4</sub> consumption by oxidation, could produce ambiguous methane isotope signals<sup>34</sup>. Nevertheless, the carbon isotope separation ( $\epsilon_{\text{C}}$ ) between CH<sub>4</sub> and CO<sub>2</sub> (defined by  $\epsilon_{\text{C}} \approx \delta^{13}\text{C}_{\text{CO}_2} - \delta^{13}\text{C}_{\text{CH}_4}$ ) can remain consistent despite large variations in the actual  $\delta^{13}\text{C}_{\text{CH}_4}$  values and indicative of the particular methanogenic pathway<sup>34</sup>. Accordingly, the  $\delta^{13}\text{C}_{\text{CH}_4}$  values in combination with the coexisting isotope information ( $\epsilon_{\text{C}}$ ) on CO<sub>2</sub> and CH<sub>4</sub> may be adequate to reliably distinguish methane sources.

Based on a 3 km<sup>2</sup> grid-monitoring results of near-surface soil samples in the Muli permafrost region<sup>35,36</sup>, a high  $\delta^{13}\text{C}_{\text{CH}_4}$  value area was observed near the gas hydrate drilling wells DK-1,2,3,7,8 from August to October, indicating the possible influence of thermogenically derived methane effusion from natural gas hydrates. In this study, a typical gas hydrate reservoir site near the well DK-8 in the Muli permafrost region of the Qilian Mountains (Fig. 1) was selected to conduct a two-year monthly field monitoring of concentrations and stable carbon isotopic compositions of CO<sub>2</sub> and CH<sub>4</sub> in near-surface soil free gas and in low-level air from January 2017 to December 2018. The hydrocarbon gases emitted from the well DK-8 was also monitored to determine the stable carbon isotopic signature of CH<sub>4</sub> and CO<sub>2</sub> effused from natural gas hydrates. This field monitoring results were aimed to provide new evidences for identifying gas hydrate release as a significant source of methane emission from the Qilian Mountains permafrost wetland, to determine the influence of gas hydrate release on methane seasonal emissions, and to facilitate understanding carbon cycling and its climate effect in the permafrost regions of the Qinghai-Tibet Plateau.

## Results

### Monthly temperature variation of the soil upper active layer.

The monthly temperature variations of the soil upper active layer and low-level air are shown in Fig. 2 based on daily monitoring average data through 2017 and 2018 at the gas hydrate drilling area in the Muli permafrost of the Qilian Mountains. The soil temperature varied with the atmospheric temperature, but had a smaller variation range than the corresponding atmospheric temperature. The soil temperature in winter had the lowest around -16°C, and the one in summer had the highest around 16°C. The soil temperature was above 0°C in summer (June-August) and below 0°C in winter (December-February), and increased gradually in spring (March-May) and decreased in autumn (September-November). The soil temperature was first observed above 0°C in the early April, but always greater than 0°C between May and October which is main period of permafrost thawing.

### Methane content and carbon isotopic composition of gas effusion from the gas hydrate drilling well DK-8.

The monthly variations in methane content and carbon isotopic composition of gas effusion from the well DK-8 during the period from January to August in 2017 are shown in Fig. 3. The measured methane contents showed a large variation from 1.904 ppm to 8.530 ppm, with the average of 2.675 ppm. The methane was constant at a low concentration of  $1.967 \pm 0.130$  ppm from January to March and of  $2.015 \pm 0.108$  ppm from June to August, whereas it increased obviously in April–May with the average of 4.409 ppm. The measured carbon isotope compositions of methane ( $\delta^{13}\text{C}_{\text{CH}_4}$ ) were between -49.6‰ and -34.6‰ with the average of -45.2‰, similar as the range of the headspace gases from gas hydrate-bearing drill cores retrieved from the depth of 104.6m to 397.99m of the DK-8 (generally from -38.3‰ to

-53.2‰ with the average of -43.6‰)<sup>23</sup>. They are characterized by less negative  $\delta^{13}\text{C}_{\text{CH}_4}$  values, which are typical of thermogenically-derived methane source (-48‰ to -35‰)<sup>33</sup>.

The monthly variation of the carbon isotopic composition was almost parallel with that of the methane content (Fig. 3a). And a positive relationship was observed between the methane contents and  $\delta^{13}\text{C}_{\text{CH}_4}$  values (Fig. 3b). Generally, the higher content of methane had less negative  $\delta^{13}\text{C}_{\text{CH}_4}$  value. The methane concentration suddenly increased to 2.920 ppm at the early April with  $\delta^{13}\text{C}_{\text{CH}_4}$  of -39.9‰, and peaked at 8.530 ppm in early May with  $\delta^{13}\text{C}_{\text{CH}_4}$  of -40.8‰, and increased to 4.201 ppm at the late May with  $\delta^{13}\text{C}_{\text{CH}_4}$  of -34.6‰. The less negative  $\delta^{13}\text{C}_{\text{CH}_4}$  values indicated that the increase of methane concentration was attributed to release of substantial proportion of accumulated gas hydrate when the temperature rised above 0°C. Samples collected in late May had the highest  $\delta^{13}\text{C}_{\text{CH}_4}$  whereas samples in June-July had the lowest  $\delta^{13}\text{C}_{\text{CH}_4}$ . The more negative  $\delta^{13}\text{C}_{\text{CH}_4}$  values in June-July indicated bacterially-derived methane that also contributed to the methane emission under the influence of elevated temperatures.

The carbon isotope separation factor ( $\epsilon_{\text{C}}$ ) between  $\delta^{13}\text{C}_{\text{CO}_2}$  and  $\delta^{13}\text{C}_{\text{CH}_4}$  of gas hydrates found in the Muli permafrost region ranged from 20‰ to 40‰, with values most commonly around 30‰ to 40‰ (Fig. 4). The  $\epsilon_{\text{C}}$  values of gas hydrates can be indicative of thermogenically-derived methane, due to the distinguishing isotopic signature from the  $\epsilon_{\text{C}}$  values associated with methanogenesis generally more than 40‰<sup>34</sup>. The  $\epsilon_{\text{C}}$  values of gas effusion from the well DK-8 ranged between 29.2‰ and 39.5‰, especially the  $\epsilon_{\text{C}}$  values in April-May closer to 30‰, further proving the release of gas hydrates. The exceptions of  $\epsilon_{\text{C}}$  values (44.4 ~ 46.3‰) in June-July were more than 40‰, also indicating the contribution of biogenic methane.

### **Methane content and carbon isotopic composition of low-level air.**

The monthly variations in methane content and carbon isotopic composition of low-level air in 2017–2018 are shown in Fig. 5a. The methane concentrations of low-level air samples ranged from 1.880 ppm to 2.048 ppm with an average of 1.933 ppm. The average of methane content was 1.933 ppm, which was slightly higher than that of the Waliguan station in Qinghai through 2017 (1.912 ppm) and significantly higher than the globally averaged methane content (1.859 ppm) reported by WMO in 2017. The  $\delta^{13}\text{C}_{\text{CH}_4}$  values of low-level air samples were between -50.4‰ and -45.9‰, with an average of -48.7‰. The  $\delta^{13}\text{C}_{\text{CH}_4}$  values in 2018 were slightly higher than in 2017. There is no significant correlation between the methane concentrations and the carbon isotopic compositions. However, samples collected in summer had higher methane concentrations with more negative  $\delta^{13}\text{C}_{\text{CH}_4}$  values. The  $\epsilon_{\text{C}}$  values of low-level air ranged from 38‰ to 46‰, with an average of 41.5‰. It is worth mentioning that the methane content and  $\delta^{13}\text{C}_{\text{CH}_4}$  value, as well as the  $\epsilon_{\text{C}}$  value exhibited consistent variation at early April, characterized by

higher CH<sub>4</sub> concentration, less negative  $\delta^{13}\text{C}_{\text{CH}_4}$  and lower  $\epsilon_{\text{C}}$  value. This reflected the effect of methane emission from the gas hydrate drilling wells on the local low-level air CH<sub>4</sub> concentration.

The methane content exhibited seasonal variation trend, with the highest mean values in summer, followed by spring and autumn, and the lowest mean values in winter (Fig. 5b). Samples collected in Summer had higher mean  $\delta^{13}\text{C}_{\text{CH}_4}$  than in spring with a wider  $\delta^{13}\text{C}_{\text{CH}_4}$  range from -50.4‰ to -47.1‰, and had the highest mean  $\epsilon_{\text{C}}$  values of 43.7‰ with a  $\epsilon_{\text{C}}$  range between 40.5‰ and 46.3‰. The carbon isotopic compositions indicate the increase of CH<sub>4</sub> concentration in low-level air was mainly contributed by biogenically derived methane. The obvious difference is that samples collected in autumn and winter had higher  $\delta^{13}\text{C}_{\text{CH}_4}$  but lower  $\epsilon_{\text{C}}$  than in summer, indicating non-negligible contribution from thermogenically derived methane.

### **Carbon isotopic composition of methane from the upper active layer of soil.**

The results show the  $\delta^{13}\text{C}_{\text{CH}_4}$  values of the upper active layer of soil through 2017 and 2018 ranging between -53.2‰ and -39.9‰ with an average of -47.7‰, and the  $\epsilon_{\text{C}}$  values ranging between 28.6‰ and 47.9‰ with an average of 40.3‰. The monthly variation trend of  $\epsilon_{\text{C}}$  values of soil samples was opposite to that of the  $\delta^{13}\text{C}_{\text{CH}_4}$  value (Fig. 6a). The  $\epsilon_{\text{C}}$  value is higher when the  $\delta^{13}\text{C}_{\text{CH}_4}$  value is lower, vice versa. This negative correlation reflects seasonal variation of methane source. Samples collected in spring and summer had lower  $\delta^{13}\text{C}_{\text{CH}_4}$  values, whereas samples collected in autumn and winter had higher  $\delta^{13}\text{C}_{\text{CH}_4}$  values (Fig. 6b). Especially, samples in winter had  $\delta^{13}\text{C}_{\text{CH}_4}$  values heavier than -50‰ and  $\epsilon_{\text{C}}$  values less than 40‰, indicating the methane was dominated by thermogenic origin.

The combination plots of  $\delta^{13}\text{C}_{\text{CH}_4}$  and  $\delta^{13}\text{C}_{\text{CO}_2}$  with isotope fractionation lines ( $\epsilon_{\text{C}}$ ) are shown in Fig. 7, differentiating the major methane sources, methanogenic pathways and methane oxidation. The carbon isotope fractionation factor for methanogenesis predominantly of carbonate reduction most commonly from 49‰ to 100‰, with values most commonly around 65‰ to 75‰, and that dominated by fermentation of methylated substrates are distinctively lower with  $\epsilon_{\text{C}}$  values typically ranging between 40‰ to 55‰<sup>34</sup>. In comparison, the methane associated with thermogenic gas hydrates emission has distinctly lower  $\epsilon_{\text{C}}$  values between 20‰ and 40‰, with the corresponding  $\delta^{13}\text{C}_{\text{CH}_4}$  values heavier than -50‰. The soil samples are plotted near the range of methane originated from methyl oxidation and gas hydrates, without noticeable CH<sub>4</sub> oxidation. Some of samples collected in spring and summer plotted in the methyl oxidation zone indicated the soil methane being dominated by methanogenic source, and the others plotted between the zone of methyl oxidation and gas hydrates indicated another contribution of thermogenic production. In contrast, samples collected in winter were almost plotted in the zone of gas hydrates, indicating the soil methane being dominated by thermogenically-derived source. The two samples in autumn showing rising  $\delta^{13}\text{C}_{\text{CH}_4}$  value and lowering  $\epsilon_{\text{C}}$  from september to october indicated a decrease in bacterial activity and an increase in thermogenic production during the transition from summer to winter.

## Discussion

The gases of thermogenic gas hydrates samples in the Muli permafrost of the Qilian Mountains had a distinctive  $\delta^{13}\text{C}_{\text{CH}_4}$  values heavier than  $-50\text{‰}$  and lower  $\epsilon_{\text{C}}$  values of  $20\text{‰}\sim 40\text{‰}$  from the bacterially-derived methane. Therefore, the isotope signatures of  $\delta^{13}\text{C}_{\text{CH}_4}$  combined with  $\epsilon_{\text{C}}$  can be adequate to reliably distinguish biogenically or thermogenically derived methane. The seasonal variation of methane sources of wetland emission and low-level air can be summarized and classified as shown in Fig. 8.

The gas effusion measured at the mouth of the well DK-8 is derived from the gas hydrates-bearing layers at a depth of 150 m  $\sim$  305 m in the Muli permafrost region, representative of deep methane upward emission. The  $\delta^{13}\text{C}_{\text{CH}_4}$  of gas effusion from the well DK-8 is typical characteristics of thermogenically-derived methane, consistent with the lower  $\epsilon_{\text{C}}$  values between  $29.2\text{‰}$  and  $39.5\text{‰}$ . The two exceptional samples with higher  $\epsilon_{\text{C}}$  of  $44.4\text{‰}\sim 46.3\text{‰}$  reflected methane contribution from biogenic sources in summer. The substantial  $\text{CH}_4$  effusion out of the gas hydrates drilling wells occurred in spring when the accumulated thermogenic methane escaped upward due to the ice melting in the upper wells. A response of local low-level air to the well emission can be found by the  $\text{CH}_4$  content increase, less negative  $\delta^{13}\text{C}_{\text{CH}_4}$  and lower  $\epsilon_{\text{C}} < 40$  during the same period. It is indicated that thermogenic methane effusion through drilling wells is an important source of local low-level air methane in spring that needs to be considered.

The combined effects of both methanogenically and thermogenically derived methane control the seasonal variation of wetland methane emission and methane content in local low-level air. This finding further suggests gas hydrate release is an important source of methane emission from wetland soils in Qilian Mountain permafrost. During spring and summer, soil temperature increase and permafrost thawing promoted flourishly growing of wetland organisms and exponentially increasing of microbial communities<sup>37-39</sup>, which can lead to an increase in biogenic methane emission. Simultaneously, the permafrost started to thaw after the soil temperature above  $0^\circ\text{C}$  in the late spring and the thawing depth peaked in July and August. The emission of thermogenic methane from subterranean gas hydrates can be accelerated through the new channels resulted from permafrost thawing. The carbon isotope compositions of  $\delta^{13}\text{C}_{\text{CH}_4}$  and  $\epsilon_{\text{C}}$  of wetland emission and low-level air consistently reflected the dynamic variation of relative contributions of biogenic and thermogenic methane during spring and summer. The air methane as well as the related soil methane conformably exhibited the lowest  $\delta^{13}\text{C}_{\text{CH}_4}$  and the highest  $\epsilon_{\text{C}}$  values when the low-level air methane concentration reached a maximum in the summer months from July to August, indicating methanogenically derived methane is the dominant source attributing to the increase in air methane concentration.

During the transition from late summer to autumn, microbial activities become weaker as the temperature decreases and consequential reduction in the methane production by methanogens. In addition, the soil temperature falls below  $0^\circ\text{C}$  since November, freezing in the permafrost leads to decreased effusion of methane from subterranean gas hydrates. As a result, low-level air methane concentrations reduce greatly and methane contributions from thermogenic source increase compared with that in summer.

During winter, the thermogenically derived methane becomes the dominant source of the wetland methane and low-level air methane, which may seep from subterranean gas hydrates through faults or drainage systems or drilled-through permafrost layers.

## Conclusions

The two-year systematic field monitoring of methane sources at a typical gas hydrate site in the Qilian Mountains permafrost provided evidence that upward effusion of natural gas hydrate underground is an important methane source of permafrost wetland and can be released into the low-level air. The carbon isotope fractionation ( $\epsilon_C$ ) between  $\text{CH}_4$  and  $\text{CO}_2$  in combination with carbon isotopic composition of methane ( $\delta^{13}\text{C}_{\text{CH}_4}$ ) is an excellent tracer to differentiate methane of thermogenic origin and microbial origin in complex environmental samples. The gas effusion of the gas hydrate drilling well DK-8 indicated methane emission from the thermogenic gas hydrates, particularly in April and May when it is the initial period of the temperature rising above 0 °C. The seasonal variation of methane sources of near-surface soil fluxes and low-level air confirmed the significance of methane emission from the thermogenic gas hydrates on local permafrost wetland methane emission as well as low-level air methane content. The thermogenically derived methane were identified as the dominant source of methane in wetland soil and low-level air in autumn and winter. The effect of gas hydrate on methane emission of the permafrost wetland may become more significant as the climate warms to accelerate dissociating the hydrate. How much impact the gas hydrate release can cause on regional wetland methane emission in the Qilian Mountains permafrost still requires more researches to fully understand.

## Methods

### Field site selection and monitoring.

The Muli gas hydrates reservoir region in the Qilian Mountains permafrost is the study area located in the northeastern Qinghai-Tibet Plateau with an altitude of approximately 4000 m to 4300 m. It is also a typical wetland dominated as alpine meadow grassland. Eight gas hydrate scientific drilling wells were drilled in 2008, and one of the drilling wells namely DK-8 was twice tested for mining gas hydrate in 2011 and 2016 respectively. The two-year field methane monitoring of near-surface soil and low-level air near the well DK-8 was conducted from January 2017 to December 2018. Methane content and stable carbon isotopic compositions of  $\text{CH}_4$  and  $\text{CO}_2$  were analyzed as well as atmospheric and near-surface soil temperatures. The gas effusion from the well DK-8 was monitored between January and August in 2017 due to the subsequent installation of in-situ hydrological monitoring equipments.

The well DK-8 is 401.05m deep, and is connected with the surrounding environment only at the depth between 150m and 305m. This means that the mixing gas in the well mainly derived from the deep under the permafrost rather than the upper 150m layers. During the monitoring period, the well DK-8 was sealed and its sampling port was connected by a teflon tubing to a Picarro G2201-I isotope analyser. The low-

level air was collected at a height of ~ 1.5m above the ground near the well DK-8, which was also connected to the isotope analyser.

### **Carbon isotope ratios of methane in near-surface soil free gas.**

A cylindrical chamber was embedded immediately in an excavated hole with a depth of 30cm at the sampling site near the well DK-8, and sealed with soil. The chamber is 53.5 cm in height and 14.4 cm in inner diameter, with several sieve holes in the buried chamber wall 10 ~ 30 cm below the ground to connect with surrounding soil. The chamber was connected to the isotope analyser by an upper sampling port. Disturbance from mixing of air and soil gas through the soil surface was assumed to be negligible because of the fine texture and compact nature of the soil and gas-tight measurement chamber.

### **In situ measurements of contents and stable carbon isotope ratios of CH<sub>4</sub> and CO<sub>2</sub>.**

On all sampling occasions, in situ CH<sub>4</sub> contents (ppm) and its  $\delta^{13}\text{C}$  values (expressed as deviation from the international standard of PDB) together with CO<sub>2</sub> were simultaneously measured using a portable Picarro isotope analyser (G2201-I; Cavity Ring-Down Spectroscopy, Picarro, USA). The Picarro analyser was checked regularly against working standards and made adjustments before the field monitoring. The sampling ports of gas effusion from the well DK-8, low-level air and near-surface soil free gas were connected respectively to three different gas inlets of the Picarro G2201-I isotope analyser. Readings were collected under a high-accuracy CH<sub>4</sub>-CO<sub>2</sub> compound mode at intervals of 5 min for a total duration of 2 hours at least. The three gas inlets were alternately switched and measured in succession for each sampling and measurement. The monitoring frequency is at least once a month. To avoid physiological fluctuation caused by gas inlet switching, the data measured during the middle 3 minutes were just used as valid data to calculate the average for each measurement. All values presented are mean  $\pm$  standard error.

## **Declarations**

### **Acknowledgements**

This study was financially supported by the open fund project of the Key Laboratory of Unconventional Oil & Gas Geology, CGS (No. DD2019137-YQ19JJ02), and the National geological survey project of China (No. DD20190102). We are grateful to the Multi Field Scientific Observation and Research Station for Gas Hydrate, China Geological Survey for the convenience and help during field work.

### **Author contributions**

S.P., designed the study and performed fieldwork; X.L., interpreted the data and wrote the paper; J.X. performed data analysis and figures drawing; Y.Z., performed fieldwork supervision; S.Z. and R.X. performed field investigation and monitoring.

# References

1. Shindell, D. T. *et al.* Improved Attribution of Climate Forcing to Emissions. *Science*. **326**, 716–718 (2009).
2. Dalsoren, S. B. *et al.* Atmospheric methane evolution the last 40 years. *Atmos. Chem. Phys.* **16**, 3099–3126 (2016).
3. Zhang, Z. *et al.* Emerging role of wetland methane emissions in driving 21st century climate change. *Proceedings Of the National Academy Of Sciences Of the United States Of America* **114**, 9647–9652(2017).
4. Zimov, S. A., Schuur, E. A. G. & Chapin, F. S. Permafrost and the global carbon budget. *Science*. **312**, 1612–1613 (2006).
5. Zimov, S. A. *et al.* Permafrost carbon: Stock and decomposability of a globally significant carbon pool. *Geophys. Res. Lett.* **33**, L20502 (2006).
6. Schuur, E. A. G. *et al.* Vulnerability of permafrost carbon to climate change: Implications for the global carbon cycle. *Bioscience*. **58**, 701–714 (2008).
7. DeConto, R. M. *et al.* Past extreme warming events linked to massive carbon release from thawing permafrost. *Nature*. **484**, 87–91 (2012).
8. Schuur, E. A. G. *et al.* Climate change and the permafrost carbon feedback. *Nature*. **520**, 171–179 (2015).
9. Knoblauch, C., Beer, C., Liebner, S., Grigoriev, M. N. & Pfeiffer, E. M. Methane production as key to the greenhouse gas budget of thawing permafrost. *Nature Climate Change*. **8**, 309–312 (2018).
10. Zhao, Z. L., Zhang, Y. L., Liu, L. S., Liu, F. G. & Zhang, H. F. Recent changes in wetlands on the Tibetan Plateau: A review. *Journal of Geographical Sciences*. **25**, 879–896 (2015).
11. Cui, M. M. *et al.* Warmer temperature accelerates methane emissions from the Zoige wetland on the Tibetan Plateau without changing methanogenic community composition. *Sci. Rep.* **5**, 11616 (2015).
12. Kuhn, M., Lundin, E. J., Giesler, R., Johansson, M. & Karlsson, J. Emissions from thaw ponds largely offset the carbon sink of northern permafrost wetlands. *Sci. Rep.* **8**, 9535 (2018).
13. Liu, W. J. *et al.* The effect of decreasing permafrost stability on ecosystem carbon in the northeastern margin of the Qinghai-Tibet Plateau. *Sci. Rep.* **8**, 4172 (2018).
14. Mu, C. C. *et al.* Greenhouse gas released from the deep permafrost in the northern Qinghai-Tibetan Plateau. *Sci. Rep.* **8**, 4205 (2018).
15. Wang, X. Q. *et al.* Response of shallow soil temperature to climate change on the Qinghai-Tibetan Plateau. *Int. J. Climatol.* **41**, 1–16 (2021).
16. Mu, C. *et al.* Editorial: Organic carbon pools in permafrost regions on the Qinghai-Xizang (Tibetan) Plateau. *Cryosphere*. **9**, 479–486 (2015).
17. Ding, J. Z. *et al.* Decadal soil carbon accumulation across Tibetan permafrost regions. *Nature Geoscience*. **10**, 420–424 (2017).

18. Mu, C. C. *et al.* The status and stability of permafrost carbon on the Tibetan Plateau. *Earth Sci. Rev.* **211**, 103433 (2020).
19. Lu, Z. Q. *et al.* Gas hydrate occurrences in the Qilian Mountain permafrost, Qinghai Province, China. *Cold Reg. Sci. Technol.* **66**, 93–104 (2011).
20. Song, Y. C. *et al.* The status of natural gas hydrate research in China: A review. *Renewable & Sustainable Energy Reviews.* **31**, 778–791 (2014).
21. Wang, X. *et al.* Reservoir volume of gas hydrate stability zones in permafrost regions of China. *Appl. Energy.* **225**, 486–500 (2018).
22. CMA. China greenhouse gas bulletin: The state of greenhouse gases in the atmosphere based on Chinese and global observations before 2017. (2018).
23. Lu, Z. Q. *et al.* Geochemistry of drill core headspace gases and its significance in gas hydrate drilling in Qilian Mountain permafrost. *J. Asian Earth Sci.* **98**, 126–140 (2015).
24. Kvenvolden, K. A. Gas hydrates - geological perspective and global change. *Rev. Geophys.* **31**, 173–187 (1993).
25. Maslin, M. *et al.* Gas hydrates: past and future geohazard? *Philosophical Transactions Of the Royal Society a-Mathematical Physical And Engineering Sciences.* **368**, 2369–2393 (2010).
26. O'Connor, F. M. *et al.* Possible role of wetlands, permafrost, and methane hydrates in the methane cycle under future climate change: a review. *Rev. Geophys.* **48**, RG4005 (2010).
27. Mestdagh, T., Poort, J. & De Batist, M. The sensitivity of gas hydrate reservoirs to climate change: Perspectives from a new combined model for permafrost-related and marine settings. *Earth Sci. Rev.* **169**, 104–131 (2017).
28. Dean, J. F. *et al.* Methane Feedbacks to the Global Climate System in a Warmer World. *Rev. Geophys.* **56**, 207–250 (2018).
29. Sun, Z. J. *et al.* Geochemical characteristics of the shallow soil above the Muli gas hydrate reservoir in the permafrost region of the Qilian Mountains, China. *J. Geochem. Explor.* **139**, 160–169 (2014).
30. Luo, M., Huang, H. G., Zhang, P., Wu, Q. H. & Chen, D. F. Origins of gas discharging from the Qiangtang Basin in the northern Qinghai-Tibet Plateau, China: Evidence from gas compositions, helium, and carbon isotopes. *J. Geochem. Explor.* **146**, 119–126 (2014).
31. Wang, P. K. *et al.* Gas hydrate stability zone migration occurred in the Qilian mountain permafrost, Qinghai, Northwest China: Evidences from pyrite morphology and pyrite sulfur isotope. *Cold Reg. Sci. Technol.* **98**, 8–17 (2014).
32. Zhang, S. Y. *et al.* Sources of seasonal wetland methane emissions in permafrost regions of the Qinghai-Tibet Plateau. *Sci. Rep.* **10**, 7520 (2020).
33. Dai, J. X. *et al.* Genetic types of gas hydrates in China. *Pet. Explor. Dev.* **44**, 887–898 (2017).
34. Whiticar, M. J. Carbon and hydrogen isotope systematics of bacterial formation and oxidation of methane. *Chem. Geol.* **161**, 291–314 (1999).

35. Zhang, F. G. *et al.* Methane emission characteristics of active layer in wetland permafrost area of the Tibetan Plateau. *Geophysical and Geochemical Exploration*. **41**, 1027–1036 (2017).
36. Zhang, S. Y. *et al.* Research on the Methane Emission and Carbon Isotope of Permafrost Wetland in Qinghai-Tibet Plateau. *Geoscience*. **32**, 1089–1096 (2018).
37. Ji, M. K. *et al.* Permafrost thawing exhibits a greater influence on bacterial richness and community structure than permafrost age in Arctic permafrost soils. *Cryosphere*. **14**, 3907–3916 (2020).
38. Mackelprang, R. *et al.* Metagenomic analysis of a permafrost microbial community reveals a rapid response to thaw. *Nature*. **480**, 368–371 (2011).
39. Chen, Y. L. *et al.* Large-scale evidence for microbial response and associated carbon release after permafrost thaw. *Global Change Biology*, online, doi:10.1111/gcb.15487, (2021).

## Figures

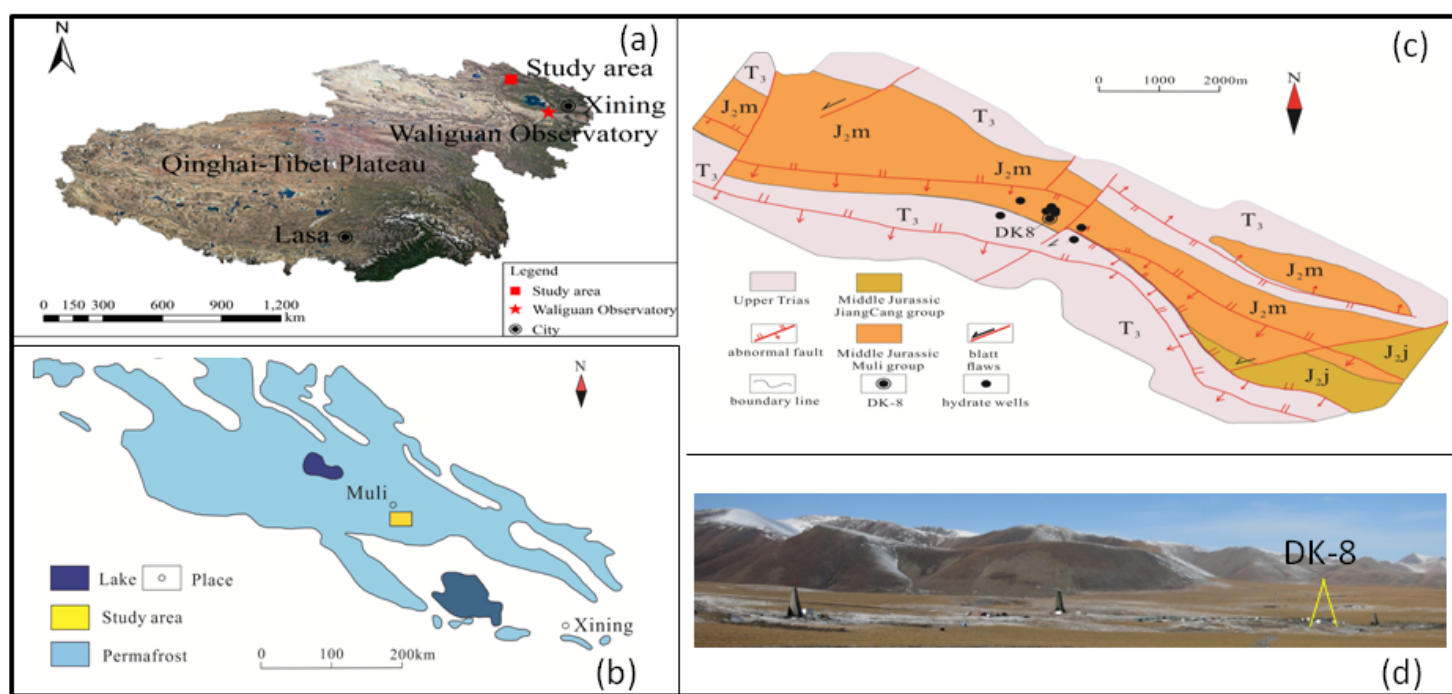


**Figure 1**

(a) Location of the study area in the Qinghai-Tibet Plateau, and (b) permafrost distribution in the Qilian Mountains, and (c) geological map showing the faults and the gas hydrate drilling wells, and (d) landscapes near the well DK-8. Note: The designations employed and the presentation of the material on this map do not imply the expression of any opinion whatsoever on the part of Research Square concerning the legal status of any country, territory, city or area or of its authorities, or concerning the delimitation of its frontiers or boundaries. This map has been provided by the authors.

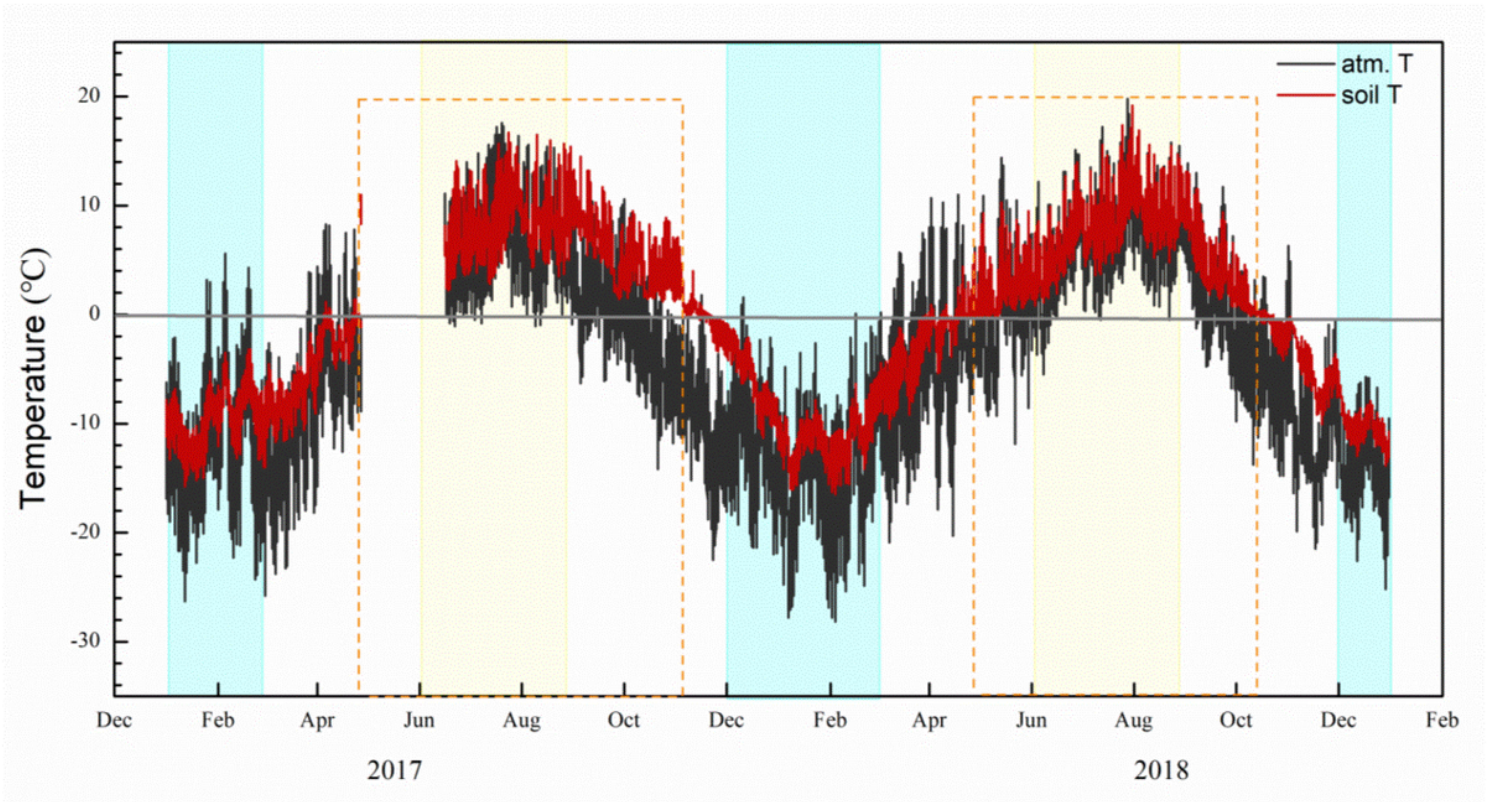


**Figure 2**

Temperature curves of low-level air and soil active layer in the Muli permafrost of the Qilian Mountains from January 2017 to December 2018.

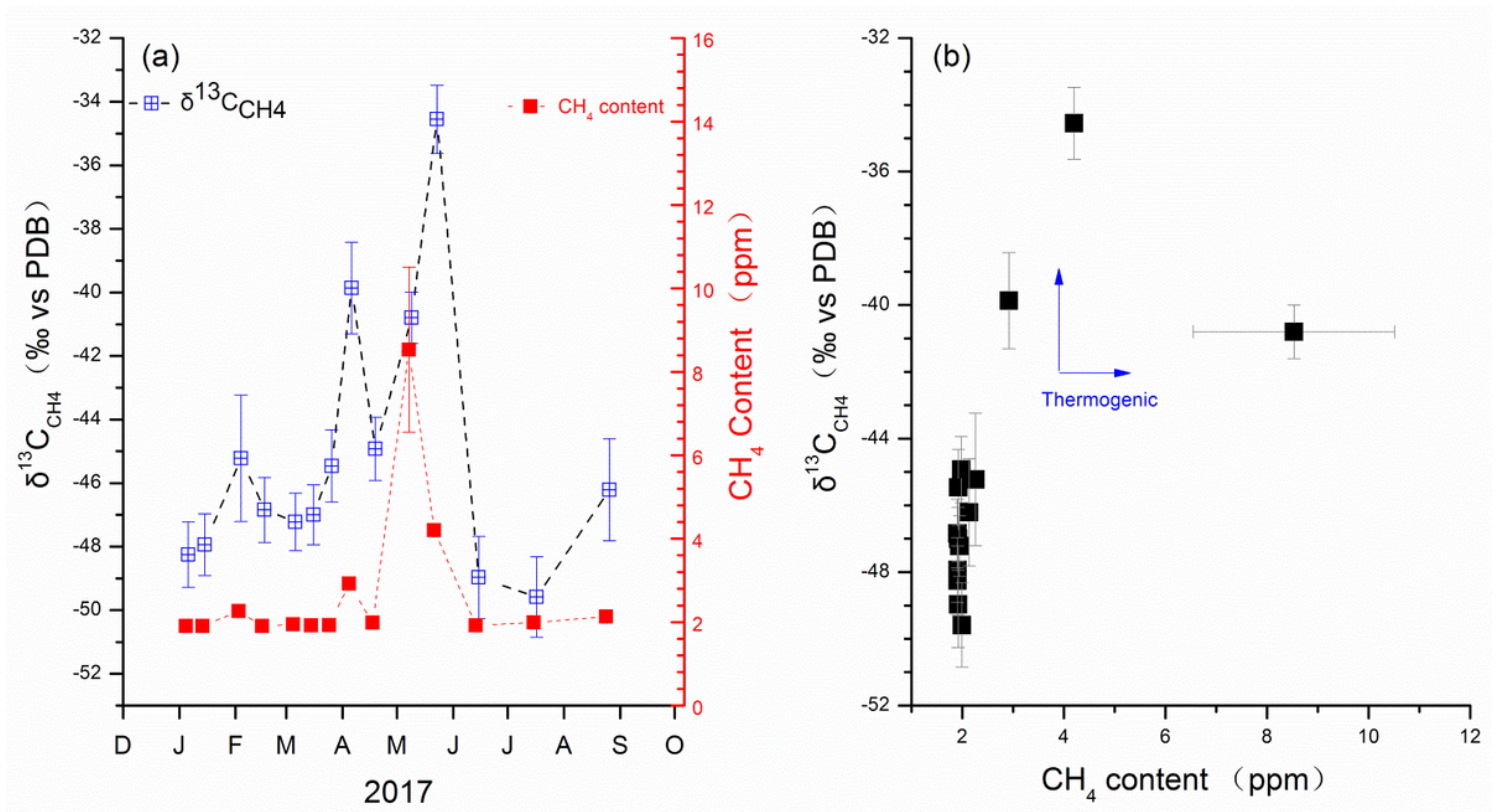


**Figure 3**

Contents and stable carbon isotopic compositions of methane effused from the gas hydrate drilling well DK-8 in 2017. (a) Monthly variation trend, and (b) correlation between stable carbon isotopic composition and content of methane.

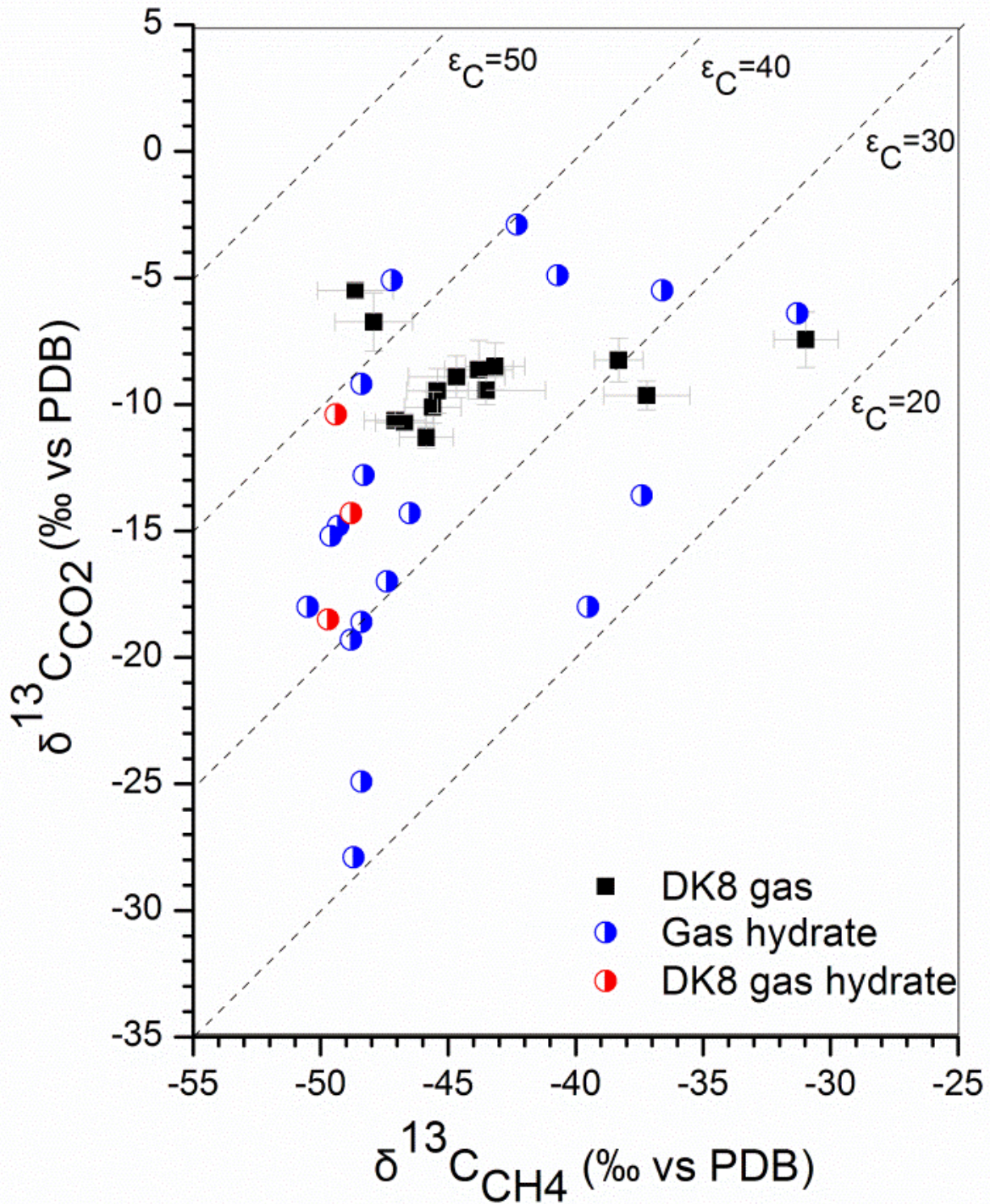


Figure 4

combination plot of  $\delta^{13}\text{C}_{\text{CH}_4}$  and  $\delta^{13}\text{C}_{\text{CO}_2}$  with isotope fractionation lines ( $\epsilon_C$ ) for gas effusion from the well DK-8 and gas hydrates found in the Muli permafrost. The carbon isotope compositions of gas

hydrates referred to Dai et al., 2017 33.

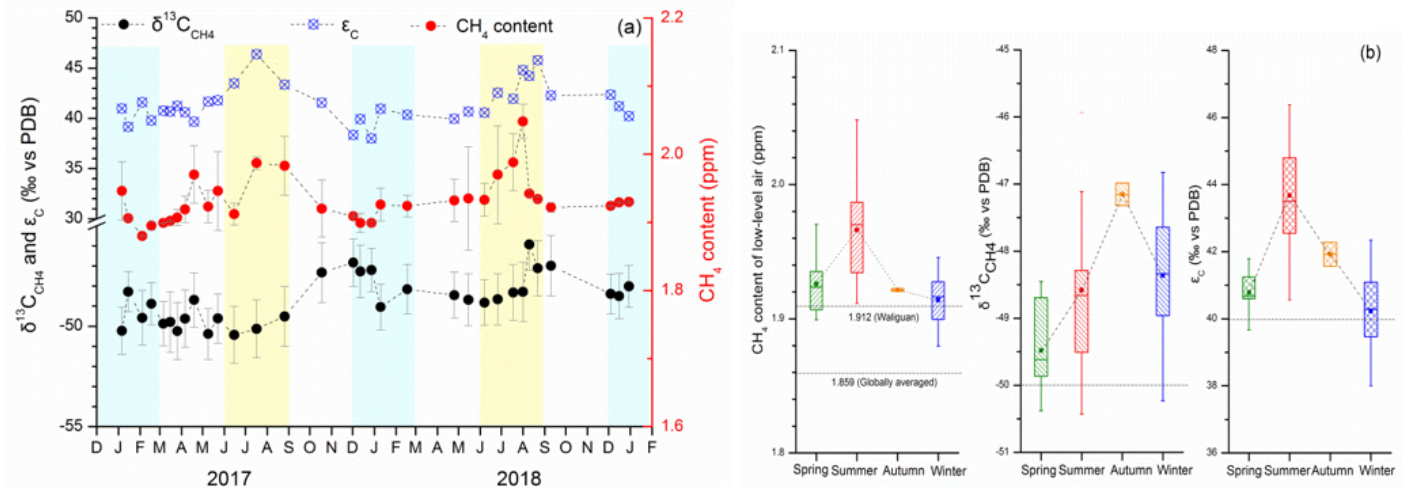


Figure 5

Content and stable carbon isotopic composition of methane and carbon isotope fractionation between  $\text{CO}_2$  and  $\text{CH}_4$  in low-level air. (a) Monthly variation of  $\text{CH}_4$  content,  $\delta^{13}\text{C}_{\text{CH}_4}$  and  $\epsilon_{\text{C}}$  values from January 2017 to December 2018. (b) Bloxplots showing seasonal variation of  $\text{CH}_4$  content,  $\delta^{13}\text{C}_{\text{CH}_4}$  and  $\epsilon_{\text{C}}$  values in low-level air. The global averaged methane and the mean methane content of Waliguan cited from CMA, 2018.

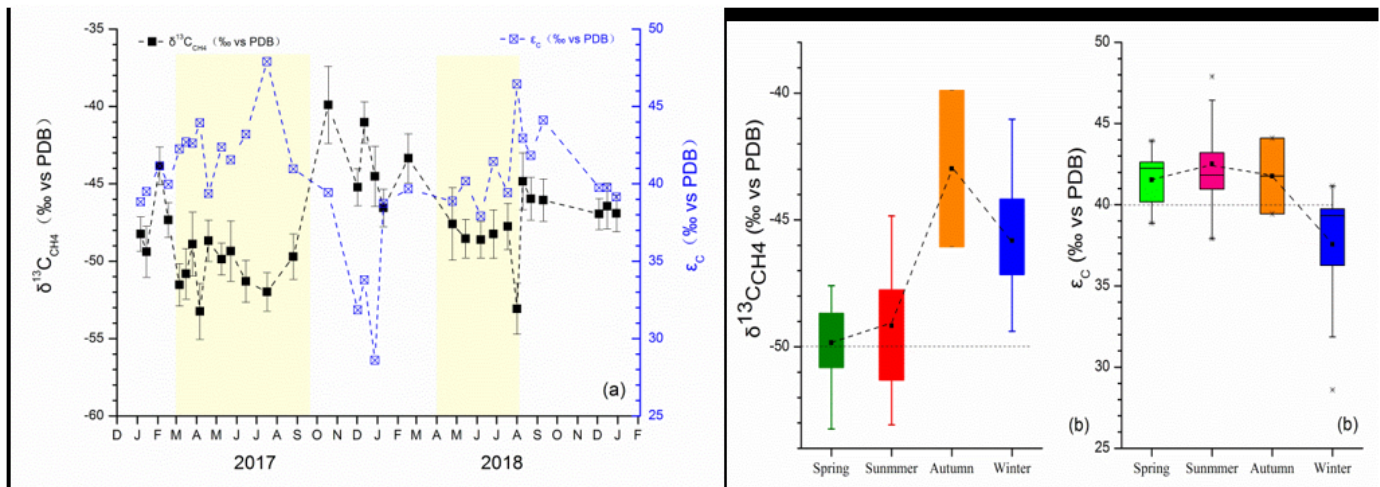
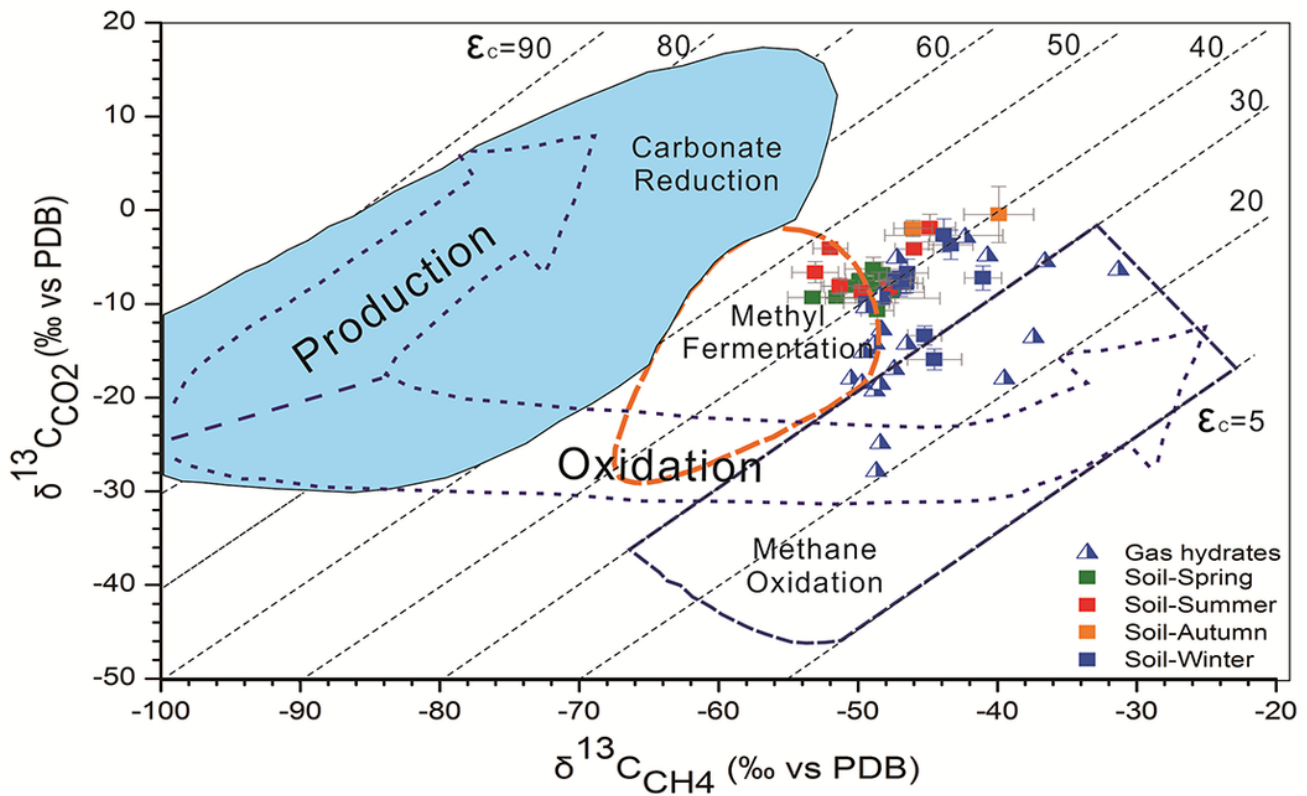


Figure 6

Stable carbon isotopic composition of methane and carbon isotope fractionation between  $\text{CO}_2$  and  $\text{CH}_4$  in the free gas of the soil active layer. (a) Monthly variation of  $\delta^{13}\text{C}_{\text{CH}_4}$  and  $\epsilon_{\text{C}}$  values from January 2017 to December 2018. (b) Bloxplots showing seasonal variation of  $\delta^{13}\text{C}_{\text{CH}_4}$  and  $\epsilon_{\text{C}}$  values in the free gas of the soil active layer.



**Figure 7**

Combination plot of  $\delta^{13}\text{C}_{\text{CH}_4}$  and  $\delta^{13}\text{C}_{\text{CO}_2}$  with isotope fractionation lines ( $\epsilon_c$ ) for the free gas of the soil active layer and gas hydrates found in the Muli permafrost region. The square in green, red, orange and blue represent the free gas of the soil active layer sampled in spring, summer, autumn and winter, respectively. The carbon isotope compositions of gas hydrates referred to Dai et al., 2017 33. The figure showing methanogenesis by carbonate reduction and methyl-type fermentation and methane oxidation refers to M.W., 1999 34.

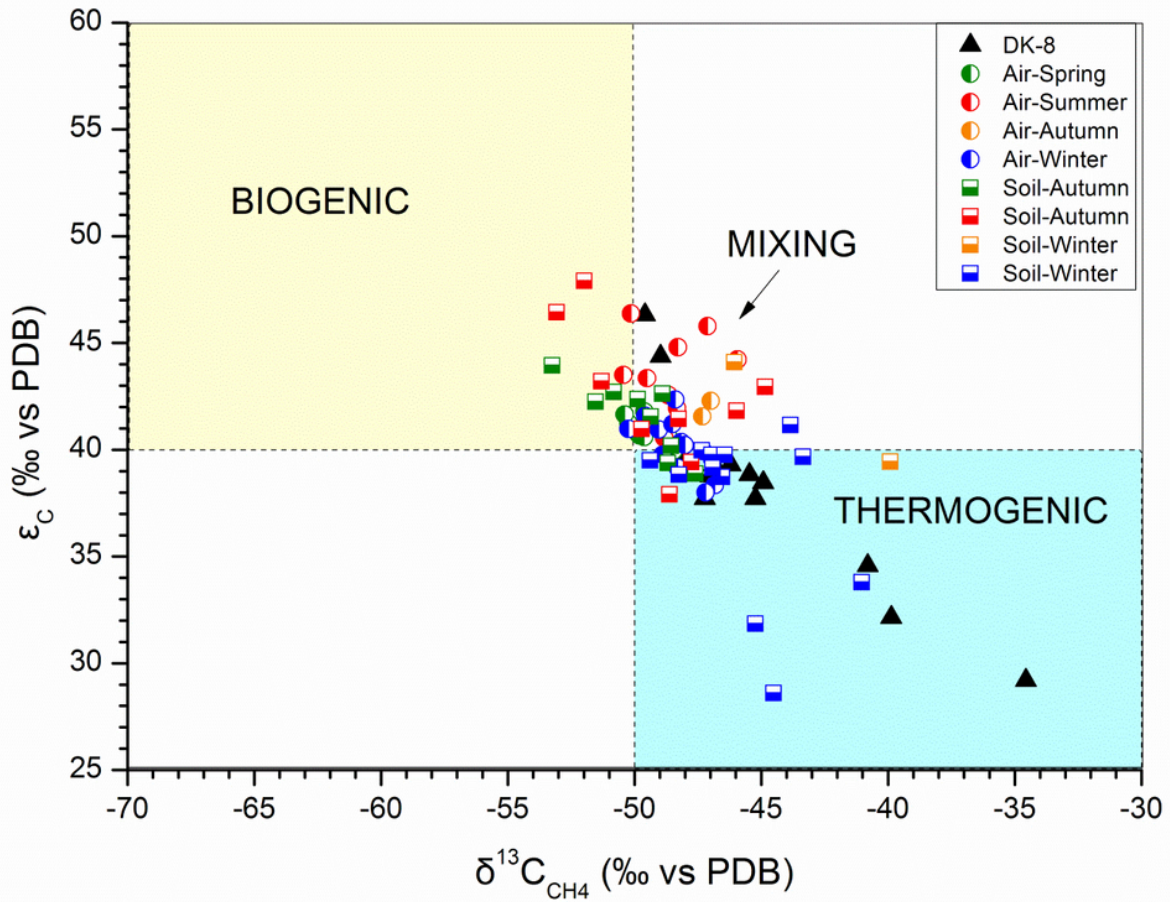


**Figure 8**

Seasonal variation of methane sources of wetland emission, low-level air and methane effusion from the well DK-8. The  $\delta^{13}\text{C}_{\text{CH}_4}$  value of  $-50$ ‰ and  $\epsilon_{\text{C}}$  value of  $40$ ‰ can be used as a threshold value to distinguish biogenically and thermogenically derived methane.